doi:10.1111/evo.13929

Feeding ecology has a stronger evolutionary influence on functional morphology than on body mass in mammals

David M. Grossnickle[1,2]

[1]*Department of Biology, University of Washington, Seattle, Washington 98195*

[2]*E-mail: dmgrossn@uw.edu*

Received September 6, 2019
Accepted January 14, 2020

Ecological specialization is a central driver of adaptive evolution. However, selective pressures may uniquely affect different ecomorphological traits (e.g., size and shape), complicating efforts to investigate the role of ecology in generating phenotypic diversity. Comparative studies can help remedy this issue by identifying specific relationships between ecologies and morphologies, thus elucidating functionally relevant traits. Jaw shape is a dietary correlate that offers considerable insight on mammalian evolution, but few studies have examined the influence of diet on jaw morphology across mammals. To this end, I apply phylogenetic comparative methods to mandibular measurements and dietary data for a diverse sample of mammals. Especially powerful predictors of diet are metrics that capture either the size of the angular process, which increases with greater herbivory, or the length of the posterior portion of the jaw, which decreases with greater herbivory. The size of the angular process likely reflects sizes of attached muscles that produce jaw movements needed to grind plant material. Further, I examine the impact of feeding ecology on body mass, an oft-used ecological surrogate in macroevolutionary studies. Although body mass commonly increases with evolutionary shifts to herbivory, it is outperformed by functional jaw morphology as a predictor of diet. Body mass is influenced by numerous factors beyond diet, and it may be evolutionarily labile relative to functional morphologies. This suggests that ecological diversification events may initially facilitate body mass diversification at smaller taxonomic and temporal scales, but sustained selective pressures will subsequently drive greater trait partitioning in functional morphologies.

KEY WORDS: **Feeding ecology, functional morphology, jaw morphology, mammal macroevolution, phylogenetic comparative methods, trait partitioning.**

A common goal in evolutionary biology is to examine the selective pressures that generate phenotypic diversity. This pursuit is complicated by numerous factors that influence morphological evolution, including stochastic processes (e.g., genetic drift and passive trends), phylogeny, biomechanics, and developmental and physiological constraints (Darwin 1859; Seilacher 1970; Raup and Gould 1974; Cheverud 1982; Lande and Arnold 1983; McShea 1994; Marroig and Cheverud 2005; Wainwright 2007; Losos 2011). Further, ecological pressures have varying effects on different morphological traits (e.g., size and shape), confounding efforts to examine adaptive evolution via analyses of morphological evolution (Marroig and Cheverud 2005; Hunt 2007; Harmon et al. 2010; Santana and Cheung 2016; Slater and Friscia 2019). These issues can be addressed in part by identifying robust correlations between ecological and morphological traits, because these associations provide strong evidence that specific ecological pressures are driving adaptive phenotypic changes. For instance, extensive studies of mammalian dentitions have shown strong associations between mammalian tooth shape and diet, including convergent morphological evolution in distantly related taxa that occupy similar ecological niches (Evans et al. 2007; Boyer 2008; Christensen 2014; Pineda-Munoz et al. 2017; Berthaume et al. 2019). This indicates that feeding ecology is a major driver of tooth shape diversification.

A further benefit of identifying strong links between ecologies and morphologies is that these associations provide critical tools for evolutionary studies, helping researchers to reconstruct paleoecologies of fossil taxa (Meng et al. 2017; Olsen 2017; Chen

et al. 2019), examine macroevolutionary patterns in major clades (Grossnickle and Polly 2013; Mitchell and Makovicky 2014), and reconstruct paleoenvironments (Vermillion et al. 2018). For instance, morphological disparity of mammalian teeth is often used as a proxy for dietary diversity, allowing studies to track ecological patterns through time and identify adaptive radiations (Osborn 1902; Simpson 1944; Van Valkenburgh 1988; Janis 1995; Jernvall et al. 1996; Wilson et al. 2012; Slater 2015; Grossnickle and Newham 2016; Slater and Friscia 2019). Body size (or body mass) is an additional morphological trait that is strongly influenced by ecology (Eisenberg 1981; Peters 1986) and is commonly used as an ecological surrogate in macroevolutionary and macroecological studies (Brown and Maurer 1989; Alroy 1999; Venditti et al. 2011; Raia et al. 2013; Saarinen et al. 2014; Huang et al. 2017). Body mass is an especially popular ecological correlate because it is often available in large-scale databases (e.g., Jones et al. 2009; Faurby et al. 2018) and readily estimated for fossil taxa (Smits 2015; Hopkins 2018). Numerous comparative studies have recently used mammalian body size evolution to examine topics such as rates of evolution, biogeographical patterns, evolutionary trends (e.g., Cope's rule), and extinction risk (Cooper and Purvis 2010; Smith et al. 2010; Smith and Lyons 2011; Uyeda et al. 2011; Venditti et al. 2011; Evans et al. 2012; Raia et al. 2012; Slater 2013; Tomiya 2013; Saarinen et al. 2014; Price and Hopkins 2015; Smits 2015; Huang et al. 2017).

A critical issue, however, is that the choice of ecological proxy can have a major influence on the conclusions of macroevolutionary studies. For instance, Slater and Friscia (2019) find evidence of an adaptive radiation (i.e., an "early burst" of ecomorphological diversification) in Carnivora via functional dental metrics that are strongly correlated with diet, but this signal is absent for additional morphological traits that have less functional relevance. Examining evolutionary patterns of nonfunctional traits may be less informative because an increase in disparity could simply reflect stochastic evolutionary changes rather than adaptive evolution (Raup and Gould 1974; McShea 1994). In addition, using body mass as an ecological proxy may be less informative than using functional morphology because many factors influence body size (Peters 1986; Cooper and Purvis 2010; Tomiya 2013; Pineda-Munoz et al. 2016), making it difficult to interpret which factors are the primary drivers of body mass evolution.

Here, I examine the influence of diet on the jaw morphology of extant therian mammals (i.e., placentals and marsupials). Therians diversified from small insectivores in the Late Jurassic–Early Cretaceous (ca. 160−100 million years ago) into one of the most functionally diverse clades on Earth, occupying an incredible array of ecological niches and possessing body masses that span eight orders of magnitude (Simpson 1944; Eisenberg 1981; Brown and Maurer 1989; Alroy 1999; Smith et al. 2010; Luo et al. 2011; Grossnickle and Newham 2016; Chen et al. 2019). Numerous therian subclades adaptively radiated in response to novel ecological opportunities, often resulting in convergent evolution of ecomorphotypes as lineages repeatedly invaded similar ecological niches or adaptive zones (Osborn 1902; Simpson 1944; Eisenberg 1981; Smith et al. 2004; Grossnickle et al. 2019). In concert with therians, flowering plants and several insect groups have diversified since the Late Cretaceous (Wing and Tiffney 1987; Collinson and Hooker 1991; Moreau et al. 2006; McKenna et al. 2009; Feild et al. 2011; Ahrens et al. 2014; Eriksson 2016), likely facilitating an immense expansion of therian diets and habitats (Janis 1995; Jernvall et al. 1996; Grossnickle and Newham 2016; Chen et al. 2019; Grossnickle et al. 2019). Thus, feeding ecology has had a major influence on mammalian diversification, and therians offer an exemplary system for examining relationships between ecology and morphology.

I examine mammalian jaw morphology because of its direct functional link to feeding ecology (Maynard Smith and Savage 1959; Turnbull 1970; Grossnickle and Polly 2013). Further, investigations of jaw morphology and diet across Mammalia are rare, especially in comparison to similar studies of mammalian tooth shape (Evans et al. 2007; Boyer 2008; Christensen 2014; Pineda-Munoz et al. 2017; Berthaume et al. 2019). And a majority of studies on mammalian jaw shape and diet are qualitative (e.g., Maynard Smith and Savage 1959), lack statistical correction for phylogenetic non-independence (e.g., Grossnickle and Polly 2013), or focus on mammalian subclades rather than all of Mammalia (Radinsky 1981; Radinsky 1985; Anapol and Lee 1994; Janis 1995; Mendoza et al. 2002; Nogueira et al. 2005; Figueirido et al. 2010; Meloro and O'Higgins 2011; Monteiro and Nogueira 2011; Ross et al. 2012; Lazagabaster et al. 2016; Maestri et al. 2016; Arregoitia et al. 2017). I incorporate data from 21 taxonomic orders of therians, thus providing insight on convergent evolutionary changes in jaw morphology across broad taxonomic groups.

In this study, I have two primary objectives. First, I establish a robust, functionally relevant correlation between ecology (i.e., diet) and morphology (i.e., jaw shape), providing a tool for examining macroevolutionary dynamics during the ecological diversification of mammals. Second, I compare the performances of functional morphology and body mass as ecological proxies in mammals. Macroevolutionary patterns of size and shape are often examined together (Marroig and Cheverud 2005; Hunt 2007; Harmon et al. 2010; Mahler et al. 2010; Wilson et al. 2012; Grossnickle and Polly 2013; Slater 2015; Slater and Friscia 2019). However, it is less common for studies to compare the impact of specific ecological pressures on these two types of traits (Santana and Cheung 2016; Zelditch et al. 2017). Body mass tends to increase with greater herbivory (Eisenberg 1981; Price and Hopkins 2015), possibly due to several benefits of greater size: decreased energy requirements (per mass unit), increased gut capacity for digestion

of plant materials, predator avoidance, and allowance for greater home ranges (Eisenberg 1981; Demment and Van Soest 1985; Peters 1986; Pineda-Munoz et al. 2016). However, the significance of the relationship between mass and diet during ecological radiations of higher-level taxa is less clear (Raia et al. 2013; Slater and Friscia 2019). Thus, this study offers novel insight on the magnitude of selective forces on multiple phenotypic traits during the radiation of therians, and results are especially relevant to future studies that use morphological traits as ecological proxies.

Methods

DIETS

Dietary information for 211 mammalian species (representing 21 taxonomic orders) was compiled and recorded as the proportion of plant (and fungal) material in the diet (Table S1). Prior to analyses, these data were arcsine-transformed, which is recommended for proportional data (Sokal and Rohlf 1995) (see Methods in the Supporting Information). Data for 186 species are from primary literature sources and based on quantitative analyses of stomach contents, building upon the dataset of Pineda-Munoz and Alroy (2014). Diets of the remaining 25 species are entirely herbivorous (100% plant material) or faunivorous (0% plant material), and sources are Nowak (1999) and the University of Michigan Museum of Zoology Animal Diversity Web (ADW) (Myers et al. 2017). All sampled species are terrestrial except for two seals (*Lobodon carcinophaga* and *Arctocephalus townsendi*), the semiaquatic capybara (*Hydrochoerus hydrochaeris*), and the semiaquatic otter shrew (*Potamogale velox*). Collecting morphometric jaw data on additional aquatic mammals is challenging because of their derived morphologies. For example, cetaceans lack distinct jaw processes and possess derived dentition (i.e., homodonty and polydonty). See Methods in the Supporting Information for additional discussion.

The percentage of plant/animal material consumed is an oversimplification of diet, especially because material and nutritional properties of plant and animal products can vary considerably (see Discussion). However, using a single, continuous dietary metric eases the computational complexity of regression and model-fitting analyses. Further, it allows strict definitions of dietary categories that are based on specific proportions of consumed foods, and this is beneficial because a majority of mammalian species consume some amount of both plant and animal matter (Pineda-Munoz and Alroy 2014), meaning that classification of species into an omnivorous category can be especially subjective. For phylogenetic one-way analyses of variance (pANOVAs) in which dietary classification in necessary, I define faunivores (or carnivores/animalivores) as species with diets consisting of 0–15% plant material ($n = 58$), omnivores as 15–85% plant material ($n = 56$), and herbivores as 85–100% plant material ($n = 97$). To test whether the choice of dietary thresholds influences results, I repeated pANOVAs using alternative dietary classifications: omnivores as 10–90% plant material consumed and omnivores as 20–80% plant material consumed (Table S5).

MORPHOLOGICAL DATA

I obtained lateral jaw images by photographing specimens in the Field Museum of Natural History collections, and I supplemented these with images from the primary literature, ADW, and Smithsonian National Museum of Natural History collections (Table S1). For most of the 211 species, I collected morphometric data for one specimen. However, for six species I collected data for 10 specimens each, and these data were used to estimate instraspecific measurement error for supplementary analyses (see below). Thus, 265 total specimens were measured. Using *ImageJ* (Schneider et al. 2012), I collected 12 linear measurements and one angle (Figs. 1 and S1; Table S2) for each jaw image. The jaw length line (measurement 1) provided a guide for subsequent measurements that are parallel or perpendicular to this line

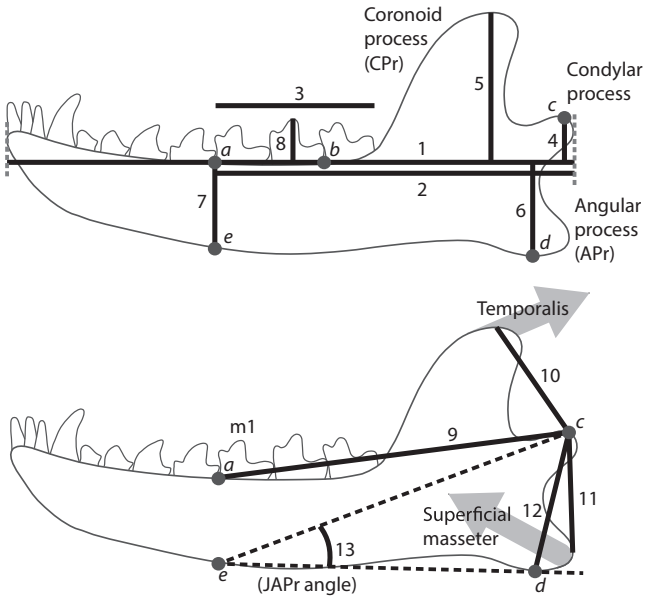

Figure 1. Mandibular measurements collected for 211 mammalian species. Measurements in the top image are perpendicular or parallel to the jaw length line (measurement 1), which passes along the alveolar margin through point *a* (between the ultimate premolar and first molar) and point *b* (between the penultimate and ultimate molars). The bottom image displays measurements involving the articulation surface of the condylar process (i.e., jaw joint, point *c*), including one angle (measurement 13). Measurements 10 and 12 approximate the moment arm lengths for the force vectors of the temporalis muscle and superficial masseter muscle, respectively. Measurement 8 is the maximum erupted height of any molar above the jaw length line. Descriptions of measurements are in Table S2. Abbreviations: JAPr angle, jaw-joint-to-angular process angle; m1, first lower molar.

(Fig. 1; Table S2). Measurement descriptions are provided in Table S2, and data are in Table S1. The jaw-joint-to-angular-process (JAPr) angle (i.e., measurement 13) is inspired by a similar measurement in Arregoitia et al. (2017), who found this angle to be correlated with diet in rodents. To address derived morphologies that make particular measurements challenging or subjective (Fig. S1), I provide additional discussion on my measurements in Methods in the Supporting Information. Adult body mass estimates are primarily from the PanTHERIA database (Jones et al. 2009), and these are supplemented with data from the ADW and primary literature (Table S1). To convert the data to a linear scale, I natural-log transformed the cube roots of the body mass estimates (Harmon et al. 2010; Slater and Friscia 2019).

To minimize variation in the morphometric data that is due to differences in jaw size among species, I size-corrected the jaw measurements prior to subsequent comparative analyses. There are benefits and drawbacks of different size-correction methods, and thus I implemented two different methods. The first method involves standardizing the linear jaw measurements by transforming them to log-shape ratios (Mosimann 1970). The log-shape ratios are calculated by dividing raw measurements by the geometric mean of all 12 linear measurements (a proxy for jaw size), and then $\log_{10}$-transforming the resulting ratio (Claude 2013; Price et al. 2019). A benefit of this method is that it preserves variation associated with allometry. Because the JAPr angle is not a linear measurement, it was simply $\log_{10}$-transformed. Converting measurements to log-shape ratios is my preferred size-correction method, and therefore the results in the main text are based on analyses that use log-shape ratios.

For the alternative size-correction method, I regressed $\log_{10}$-transformed measurements against $\log_{10}$-transformed jaw length (measurement 1) using phylogenetic generalized least squares (PGLS) regressions (Grafen 1989) via the *nlme* package (Pinheiro et al. 2016) for R software (R Core Team 2016). Residuals from the regression models were then used in all subsequent comparative analyses, and results are reported in Results in the Supporting Information. For this method, the JAPr angle was treated in the same manner as linear measurements. Because the PGLS regression model is fit while simultaneously estimating Pagel's lambda via maximum likelihood (Revell 2010), a benefit of this method is that it incorporates phylogenetic relationships and phylogenetic signal into the size correction process (Revell 2009; Price et al. 2019). However, drawbacks include the removal of variation associated with allometry (Mosimann 1970) and the elimination of jaw length as a trait that can be used in subsequent analyses.

PHYLOGENETIC COMPARATIVE METHODS

To help account for the nonindependence of data due to varying levels of phylogenetic relatedness among species, I used phylogenetic comparative methods to examine the association between morphology and diet in mammals. Due to uncertainty of the topology and branch lengths of the mammalian phylogeny, I repeated all analyses for 20 species-level phylogenetic trees from Upham et al. (2019). The trees were drawn randomly from the posterior distribution. Each tree was pruned to the species in this study, and statistical results are means of the 20 iterations.

To analyze the relationship between diet and morphology, I first used bivariate PGLS regressions (via the *nlme* R package) to predict diets (i.e., arcsine-transformed proportion of dietary plant material) using the size-corrected jaw measurements, jaw size (i.e., the geometric mean of all linear measurements), and body mass. Further, I performed a multiple PGLS regression in which jaw traits and body mass are predictor variables in a single model. However, there is considerable multicollinearity among the jaw measurements, which violates an assumption of multiple regressions and can generate spurious results (Graham 2003; see Results in the Supporting Information). Thus, bivariate regressions are preferred here.

A potential concern with using continuous dietary data in comparative analyses is that species' diets may vary considerably among populations or across seasons, especially in omnivores. Thus, I supplemented the PGLS regressions by using simulation-based pANOVAs (Garland et al. 1993) to test for statistical differences among three discrete dietary groups (i.e., faunivores, omnivores, and herbivores), with omnivores grouped together into a single, broad dietary category (15–85% plant consumption for primary analyses). Analyses were performed via the *phylANOVA* function in the *phytools* R package (Revell 2012) using 1000 simulations, and I repeated pANOVAs using alternative dietary definitions (i.e., different plant consumption percentages) to test for sensitivity of results to these definitions (Table S5).

I examine univariate jaw traits rather than perform multivariate analyses of overall jaw shape (e.g., via geometric morphometrics; Grossnickle and Polly 2013) because a central goal is to identify simple correlates of diet that can be readily applied to evolutionary model-fitting analyses (see below). Further, univariate metrics may be especially valuable to future paleontological studies because fossil jaws are often incomplete, impeding multivariate analyses of jaw shape. A potential concern with performing many bivariate comparisons between diet and morphological traits is that it increases the chance of encountering Type I error. However, my goal is not to determine statistical significance via specific *P*-values. Instead, I am investigating the relative strength of correlations between diet and various jaw traits, with a focus on how the results for jaw metrics compare to those for body mass.

MODELING ECOMORPHOLOGICAL EVOLUTION

To further examine the influence of diet on mammalian morphology, I fit seven evolutionary models to jaw and body mass

data. Goodness-of-fit was evaluated using small-sample-corrected Akaike information criterion (AICc) values (Akaike 1974; Hurvich and Tsai 1989) and relative Akaike weights. AICc calculations are based on maximum likelihood values and penalize increased model complexity. I fit uniform, two-regime, and three-regime models to the data. Uniform models include a single set of parameters applied across the entire phylogeny, and multi-regime models allow parameters to vary among taxa of different selective regimes (i.e., dietary categories in this study). To fit two-regime models, I first categorized extant species and ancestral nodes into two selective regimes: (i) plant-dominated diet (i.e., greater than 50% of diet is plant material; "herbivore") and (ii) animal-dominated diet (i.e., less than 50% of diet is plant material; "faunivore"). Diets at ancestral nodes were inferred using continuous data (i.e., proportion of plant material in diet) with the *ace* function of the *ape* package (Paradis et al. 2004), and using the default settings of residual maximum likelihood and a Brownian motion (BM) model of evolution. From these results, the ancestral nodes were assigned to the herbivory regime (>50% plants) or faunivory regime (<50% plants). To fit three-regime models, I repeated this procedure for three dietary regimes: herbivory (85–100% plants), omnivory (15–85% plants), and faunivory (0–15% plants).

Six models were fit using the *OUwie* function within the *OUwie* R package (Beaulieu and O'Meara 2016). A uniform BM model (BM1) with a single phylogenetic mean (θ) serves as the null hypothesis, and it models a constant evolutionary rate (σ^2) under the assumption of stochastic evolutionary change from a central tendency. The second model is a single-optimum Ornstein-Uhlenbeck (OU) model (Hansen 1997; Butler and King 2004). OU models include an additional parameter, α, which represents the strength of attraction toward a trait optimum (θ). Support for the BM1 or OU1 models would indicate that dietary category does not strongly influence evolutionary changes in jaw morphology or body mass. Four multi-regime models test the presence of distinct selective regimes by allowing parameters to vary among taxa of different dietary categories. Support for multi-regime models would provide evidence for the hypothesis that diet drives evolutionary changes in jaw morphology, suggesting the presence of adaptive zones (Simpson 1944) or adaptive peaks of a fitness landscape (Wright 1932) that are associated with each regime. Multi-regime models include two-regime and three-regime BM models (BMS2 and BMS3, respectively), which allow the phylogenetic means (θ) and evolutionary rates (σ^2) to vary among dietary categories. The "root station" was set to allow phylogenetic means to vary, invoking the group mean model of Thomas et al. (2006). Further, I fit two-regime and three-regime OU models (OUM2 and OUM3, respectively), which allow θ to vary among dietary groups, but α and σ^2 are kept constant across regimes. Support for the multi-regime OU models would suggest the presence of selection for trait optima. In contrast, multi-regime BM models do not model a mechanism for shifts between selective regimes. Rather, changes in diet are modeled as instantaneous shifts. Multi-regime BM models may seem counterintuitive—rapid morphological change during regime shifts suggests the presence of strong selective pressures, but BM evolutionary processes imply a lack of strong selective pressures within the regimes. One potential mechanism for generating a multi-regime BM pattern is the presence of fluctuating phylogenetic means (e.g., nonstationary adaptive peaks) through time, which might drive short-term directional changes within individual lineages but result in overall BM patterns at broader taxonomic and temporal scales (Revell et al. 2008).

The seventh model fit to the data is the early burst (EB) model (Harmon et al. 2010), which is often used to test for adaptive radiations that involve greater morphological diversification early in a clade's history. It was fit using the *fitContinuous* function in the package *geiger* version 2.0 (Pennell et al. 2014). The EB model incorporates a parameter that represents the exponential decrease in morphological rate of evolution through time. Greater morphological partitioning is expected over time, increasing the phylogenetic signal relative to BM, which is the opposite effect of an OU process (Harmon et al. 2010).

Measurement error, including intraspecific variation, can affect modeling results by reducing phylogenetic signal in datasets (Revell et al. 2008). To examine the influence of measurement error on evolutionary modeling analyses, I repeated analyses after assigning standard error values to taxa. Error values for jaw metrics were estimated by measuring 10 specimens of six species from different taxonomic orders (see Methods in the Supporting Information). For body mass, I used a standard error of 0.0345 for all mammals (*sensu* Harmon et al. 2010).

RODENTS VERSUS NONRODENTS

Comparative analyses were repeated for subsamples consisting of nonrodents ($n = 140$) and rodents ($n = 71$). Rodents were analyzed separately because they possess derived masticatory features, such as ever-growing incisors, unique jaw musculature (e.g., Cox and Baverstock 2016), and the propensity to use proal (i.e., forward) jaw movement during occlusion (rather than orthal or transverse occlusion that is common in nonrodents; von Koenigswald et al. 2013), and these traits may result in unique selective pressures and evolutionary trends. Further, rodents account for a large portion of the overall sample (and approximately 45% of all known mammalian species), and performing analyses with and without rodents allows for consideration of their influence on the overall patterns for mammals. The pANOVAs and three-regime model-fitting analyses were not performed for the rodent sample because there are only two faunivorous species when using three dietary categories.

Results

The correlation analyses identify several jaw and molar traits that are significantly associated with diet (Tables 1, S3, S4, and S8), and the best performing metrics are summarized via conceptualized jaw images for nonrodents (Fig. 2A) and rodents (Fig. 2C). Especially powerful predictors of diet are metrics that capture either the size of the angular process, which increases with greater herbivory, or the length of the posterior portion of the jaw, which decreases with greater herbivory. These metrics show significant correlations with diet in bivariate PGLS regressions, multiple PGLS regression, and pANOVAs (Tables 1, S3, S4, and S8). The overall jaw size (i.e., the geometric mean of the linear measurements) tends to increase with greater herbivory, especially in nonrodents.

Figure 3 displays frequency data for the mammalian sample and a phylogenetic tree (Upham et al. 2019) with mammals classified into two dietary regimes (i.e., faunivory and herbivory). JAPr angles have a bimodal distribution that largely separates faunivores and herbivores (Fig. 3C), and JAPr distances and jaw-joint-to-m1 distances display similar bimodal distributions (Fig. S2). The herbivores include a considerable number of rodents. However, rodents alone cannot account for the distinct jaw patterns for faunivores and herbivores, as there remains a strong correlation between the jaw metrics and diet in nonrodents (Table 1). The herbivores with relatively small JAPr angles (i.e., those overlapping with faunivores in Fig. 3C) include many fruit bats, suggesting that Chiroptera may not adhere to the trend of greater JAPr values with increased herbivory. However, I performed an independent PGLS regression for bats ($n = 30$), and results are consistent with the overall mammalian sample: diet is significantly correlated with JAPr angle (mean $t = 2.62$, mean $P = 0.015$). Thus, despite the relatively small JAPr angles, there remains a tendency toward greater JAPr angles with increased herbivory (see the example chiropteran jaws in Fig. 3B).

In evolutionary model-fitting analyses, I chose to focus on three jaw metrics with especially strong relationships to diet: JAPr distance (measurement 12), JAPr angle (measurement 13), and jaw-joint-to-m1 distance (measurement 9). Two-regime models outperform three-regime and uniform models for both the mammal and nonrodent samples (Tables 2 and S6; Fig. 4). JAPr angles for nonrodents are an exception, but Akaike weights for BMS2 and OUM2 are similar to that for BMS3. The dominant support for two-regime models is maintained when measurement error is incorporated into the model-fitting analyses (Table S7), and when PGLS regression residuals are used as an alternative method for size-correcting the linear measurements (Table S9; Fig. S4).

Although OUM2 models best fit the jaw metrics (Table 2; Fig. 4), there are concerns with using OU models in these analyses. OU models are prone to overfitting (Cooper et al. 2016), and the strong phylogenetic signals for jaw traits (Table 1) contradict an OU process, which decreases the phylogenetic signal with time. Further, the phylogenetic half-lives ($\ln(2)/\alpha$) of the jaw metrics are each approximately 40 million years. This suggests that if an OU process is occurring, dietary shifts in lineages are associated with slow rates of morphological change and/or weak selective pressures. However, in many analyses, especially those in which regression residuals were used for size correction (Table S9; Fig. S4), the additional two-regime model, BMS2, outperforms the BM1 and BMS3 models. Thus, if OU models were excluded from analyses, there would still be support for the presence of distinct faunivory and herbivory regimes via the BMS2 model.

Body mass is strongly associated with diet, especially in nonrodents (Table 1; Fig. 2). There is a general trend toward greater body size with increased herbivory, consistent with analyses in previous studies (Demment and Van Soest 1985; Price and Hopkins 2015; Pineda-Munoz et al. 2016). Faunivores and omnivores have similar average body masses (Fig. 2), but variances and evolutionary rates may be distinct between these groups (Tables 2 and S6; Price and Hopkins 2015). Evolutionary model-fitting results for body mass vary among mammals, nonrodents, and rodents (Tables 2 and S6; Figs. 3 and 4). In the mammalian sample, body mass is best explained by the three-regime BMS3 model that includes a distinct adaptive peak for omnivory (which is absent for jaw morphology), but this result is not maintained for nonrodents and rodents.

Discussion

THE INFLUENCE OF DIET ON JAW MORPHOLOGY

Diet has a powerful evolutionary influence on functional jaw morphology, and two jaw traits show especially strong relationships with diet. The first trait is the size of the angular process, which increases with greater herbivory (Tables 1, S3, and S4; Fig. 2). Of the measurements that capture angular process size (Fig. 1), the two strongest predictors of diet are the JAPr distance measured to the ventral-most margin (measurement 12) and the JAPr angle (measurement 13). The strong link between JAPr metrics and diet is consistent with qualitative observations (Maynard Smith and Savage 1959) and an analysis of jaw shape in Grossnickle and Polly (2013), which found the JAPr distance to account for much of the variation between small-mammal faunivores and herbivores.

The second jaw trait that is a powerful predictor of diet is the length of the posterior portion of the jaw, which decreases with greater herbivory (Tables 1, S3, and S4; Fig. 2). This is best captured by the jaw-joint-to-m1 distance (measurement 9) and m1-to-posterior jaw length (measurement 2). Measurements 2 and 9 do not extend anterior to m1 and are more strongly correlated

Table 1. Summary statistics for phylogenetic one-way analyses of variance (pANOVAs) and bivariate phylogenetic generalized least squares (PGLS) regressions, which examine the relationship between diet and jaw morphology in mammals.

		pANOVA		PGLS					
	Trait	*F*-stat.	*P*-value	Est.	SE	*t*-stat.	*p*-value	AIC	λ
Mammalia	1) Jaw length	27.295	0.002	−2.488	0.518	−4.805	<0.001	189.00	0.976
($n = 211$)	2) m1 to post. jaw	42.316	0.001	−3.139	0.567	−5.535	<0.001	184.43	0.963
	3) Molar row	15.647	0.022	−1.100	0.359	−3.067	0.003	202.25	0.978
	4) Joint elevation	4.872	0.262	0.301	0.138	2.174	0.033	208.40	0.983
	5) CPr elevation	7.811	0.131	0.263	0.353	0.747	0.463	210.65	0.984
	6) APr depth	23.036	0.005	0.228	0.099	2.296	0.024	208.69	0.980
	7) Corpus depth	14.303	0.029	0.664	0.381	1.744	0.087	208.09	0.981
	8) Molar depth	62.432	0.001	−1.280	0.240	−5.328	<0.001	187.20	0.967
	9) Joint to m1	50.260	0.001	−3.369	0.626	−5.379	<0.001	185.57	0.963
	10) JCPr	21.359	0.006	−0.725	0.304	−2.386	0.019	205.89	0.983
	11) JAPr post.	19.865	0.008	0.457	0.437	1.044	0.301	209.71	0.983
	12) JAPr ventral	49.387	0.001	2.418	0.437	5.535	<0.001	183.91	0.968
	13) JAPr angle	53.347	0.001	1.667	0.266	6.263	<0.001	178.94	0.961
	Body mass	9.336	0.095	0.205	0.056	3.668	<0.001	201.93	0.980
	Jaw size (GM mean)	10.691	0.065	0.008	0.002	3.166	0.002	211.46	0.978
Nonrodents	1) Jaw length	10.751	0.019	−2.182	0.663	−3.289	0.001	166.45	0.983
($n = 140$)	2) m1 to post. jaw	29.217	0.001	−2.820	0.695	−4.057	<0.001	162.41	0.970
	3) Molar row	10.540	0.020	−2.154	0.437	−4.946	<0.001	158.21	0.989
	4) Joint elevation	3.085	0.269	0.359	0.159	2.255	0.027	174.65	0.987
	5) CPr elevation	0.899	0.668	0.509	0.548	0.929	0.357	176.35	0.988
	6) APr depth	12.643	0.011	0.246	0.112	2.188	0.031	175.77	0.983
	7) Corpus depth	2.711	0.316	0.270	0.494	0.546	0.589	177.12	0.986
	8) Molar depth	39.168	0.001	−2.020	0.287	−7.050	<0.001	138.12	0.963
	9) Joint to m1	30.153	0.001	−2.979	0.776	−3.839	<0.001	163.43	0.973
	10) JCPr	12.693	0.011	−0.906	0.421	−2.151	0.034	173.18	0.985
	11) JAPr post.	6.651	0.070	0.652	0.520	1.248	0.218	175.77	0.986
	12) JAPr ventral	28.663	0.001	2.415	0.497	4.856	<0.001	156.72	0.971
	13) JAPr angle	33.722	0.001	1.646	0.305	5.404	<0.001	154.00	0.963
	Body mass	16.420	0.004	0.239	0.069	3.477	0.001	169.78	0.984
	Jaw size (GM mean)	18.788	0.003	0.008	0.003	2.760	0.007	180.49	0.982

(Continued)

Table 1. Continued.

		pANOVA		PGLS					
	Trait	*F*-stat.	*P*-value	Est.	SE	*t*-stat.	*p*-value	AIC	λ
Rodents	1) Jaw length			−3.584	0.733	−4.889	<0.001	9.18	0.835
($n = 71$)	2) m1 to post. jaw			−4.834	0.938	−5.153	<0.001	8.06	0.788
	3) Molar row			1.443	0.506	2.851	0.006	21.79	0.923
	4) Joint elevation			−0.093	0.329	−0.283	0.781	29.68	0.932
	5) CPr elevation			0.238	0.391	0.610	0.549	29.05	0.924
	6) APr depth			−0.101	0.295	−0.355	0.731	29.84	0.931
	7) Corpus depth			1.651	0.566	2.920	0.005	21.02	0.901
	8) Molar depth			0.684	0.367	1.866	0.079	26.26	0.945
	9) Joint to m1			−5.254	1.020	−5.153	<0.001	8.69	0.762
	10) JCPr			−0.458	0.389	−1.178	0.258	28.05	0.927
	11) JAPr post.			−0.746	0.833	−0.896	0.377	27.11	0.929
	12) JAPr ventral			2.090	1.192	1.753	0.085	24.40	0.902
	13) JAPr angle			1.773	0.683	2.594	0.012	22.55	0.877
	Body mass			0.132	0.096	1.380	0.175	30.36	0.922
	Jaw size (GM mean)			0.014	0.009	1.650	0.106	34.326	0.929

Note. Prior to analyses, linear jaw measurements were converted to log-shape ratios, JAPr angles were $\log_{10}$-transformed, and body masses were converted to a linear scale (see Methods). Trait numbers correspond to measurements in Figure 1 and Table S2. Results are means of replicate analyses using 20 phylogenetic trees (Upham et al. 2019). Phylogenetic signal is assessed using Pagel's lambda (λ). Rodent-only pANOVAs were not performed due to a dearth of faunivores in the sample. Abbreviations: AIC, Akaike information criterion; APr, angular process; CPr, coronoid process; Est., estimate; *F*-stat., *F*-statistic; GM, geometric mean; JAPr, joint-to-angular process; JCPr, joint-to-coronoid process; m1, first lower molar; post., posterior, SE, standard error; *t*-stat, *t*-statistic.

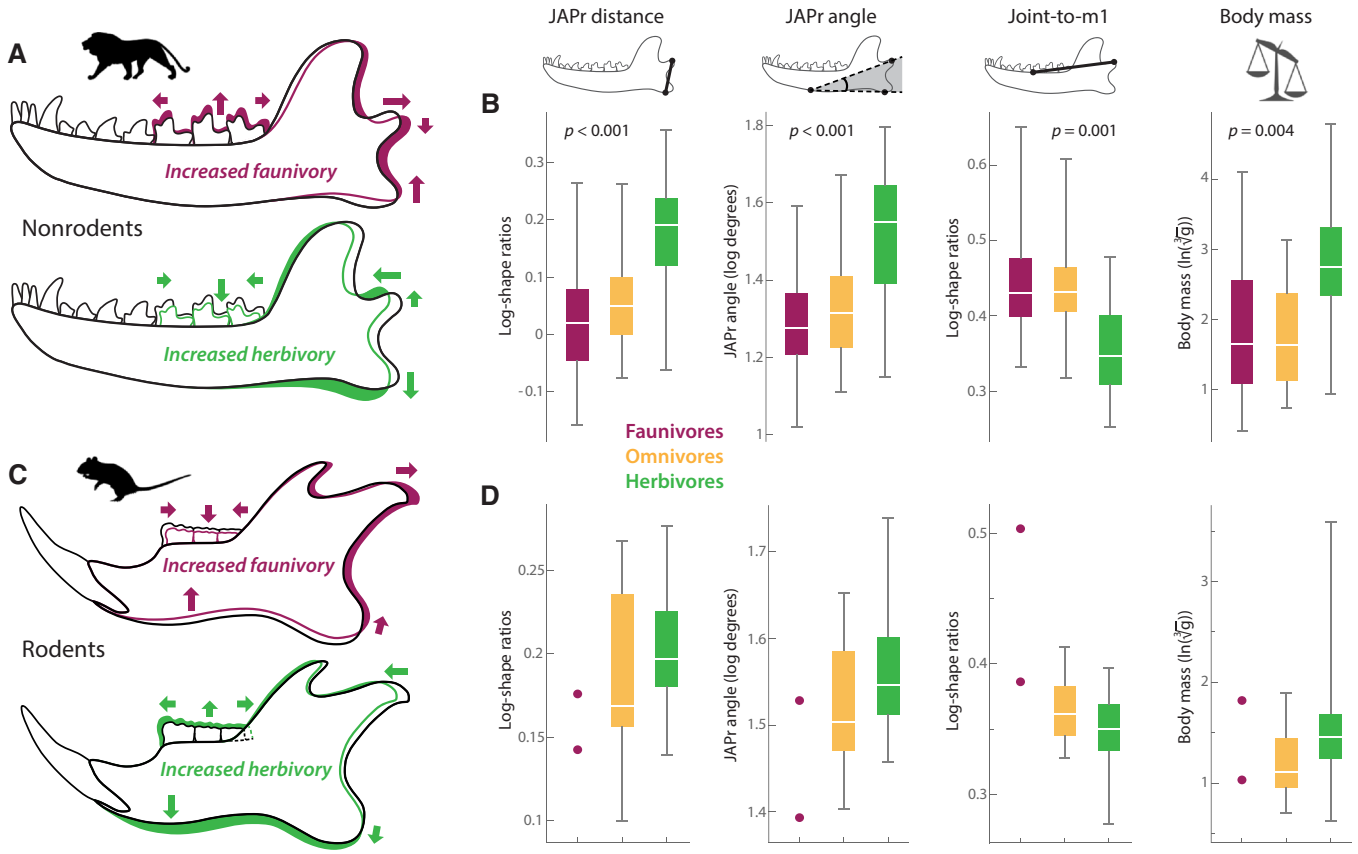

Figure 2. Schematic jaw images of nonrodents (*A*) and rodents (*C*), displaying major morphological changes that are driven by differences in diet. The arrow lengths and relative sizes of jaw changes approximate the strength of correlations between jaw metrics and diet (Table 1). *B* (nonrodents) and *D* (rodents) display jaw-joint-to-angular process (JAPr) ventral distances (measurement 12), JAPr angles (measurement 13), jaw-joint-to-m1 distances (measurement 9), and body masses for species classified into three dietary categories (see Methods). Linear jaw measurements were converted to log-shape ratios prior to analyses. The *p*-values in nonrodent plots are from pANOVAs (Table 1). Box-and-whisker plots display medians, 25% to 75% quantiles (boxes), and ranges (whiskers). Mammal silhouettes are from PhyloPic (phylopic.org).

with diet than total jaw length (measurement 1), suggesting that diet influences the posterior length of the jaw to a greater degree than it influences the anterior length. These results indicate that the jaw joint is relatively closer to m1 in herbivores (Fig. 2). However, unlike JAPr metrics, the strong correlation between posterior jaw length and diet is not maintained in analyses using the alternative size-correction method that involves PGLS regression residuals (Table S8; see Methods). In contrast to log-shape ratios (my primary method for size correction), regression residuals eliminate variation associated with allometric relationships between jaw traits and jaw length. This suggests that the correlation between posterior length of the jaw and diet (via log-shape ratios) is due in part to overall jaw size (i.e., the geometric mean) tending to increase with greater herbivory. This is because jaw size serves as the denominator in the log-shape ratios, and larger jaw sizes in herbivores will result in smaller ratios for measurements such as the posterior jaw length that do not increase with greater herbivory. This interpretation is supported by PGLS and pANOVA results for the geometric mean of jaws, which shows a strongly significant correlation with diet (Table 1), indicating that the relative jaw size (but not length) in mammals increases with herbivory. This increase in jaw size with herbivory may be driven in part by the significantly increased size of the angular process in herbivores.

The jaw-joint-to-m1 distance approximates the outlever length for bites at m1 that involve jaw rotation around an axis at the jaw joint, and mechanical advantage will increase with a shortened outlever (if the inlever remains constant). Thus, one potential biomechanical explanation for the strong correlation with diet is that the joint-to-m1 distance remains short (relative to overall jaw size) in herbivores to help maintain mechanical advantage for mastication involving cheek teeth.

Nonrodents and rodents show distinct morphological trends, especially for dentition-related traits (Fig. 2; Table 1). The molar

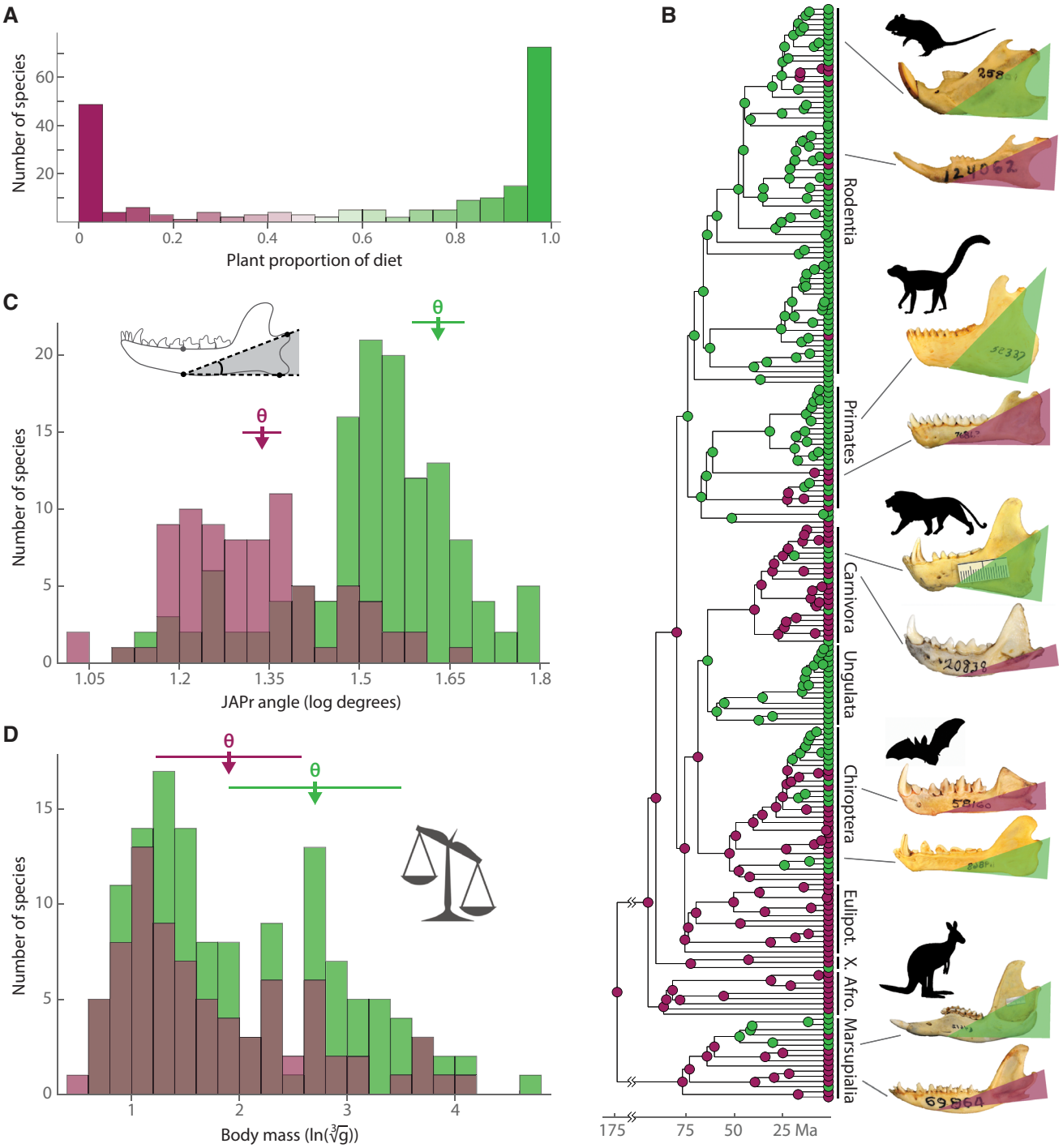

Figure 3. Selective regimes for animal-dominated diets ('faunivory'; maroon) and plant-dominated diets ('herbivory'; green), defined by the proportion of plant material in diets (*A*; Table S1). *B*, Mammalian phylogeny (from a sample of 20 trees used in this study; Upham et al. 2019) with ancestral state reconstructions at nodes, and exemplar faunivore and herbivore jaws of five mammalian clades. Triangles depict JAPr angles, highlighting the greater angle magnitudes in herbivores. Histograms of JAPr angles (*C*) and body masses (*D*) display frequency of faunivorous species and herbivorous species (brown represents overlap of the two diets). Arrows mark the trait optima or phylogenetic means (θ) from the best-fitting two-regime models, and error bars are ±1 standard error (Table 2). Jaws in *B* are from the Field Museum of Natural History (Table S1) and, from top to bottom, are *Otomys irroratus*, *Geoxus valdivianus*, *Callicebus personatus*, *Tarsius bancanus*, *Potos flavus*, *Mustela nivalis*, *Vampyrum spectrum*, *Pteropus alecto*, *Macropus giganteus*, and *Marmosa demerarae*. Silhouettes are from PhyloPic (phylopic.org). Abbreviations: Afro., Afrotheria; Eulipot., Eulipotyphla; JAPr, jaw-joint-to-angular process; Ma, millions of years ago; X., Xenarthra.

Table 2. Fits of evolutionary models to mammalian JAPr distances (measurement 12), JAPr angles (measurement 13), jaw-joint-to-m1 distances (measurement 9), and body masses.

	Model	σ^2 (1)	σ^2 (2)	σ^2 (3)	α	θ (1)	θ (2)	θ (3)	SE (1)	SE (2)	SE (3)	A. wt.
JAPr distance	BM	0.0001	–	–	–	0.118	–	–	0.076	–	–	0.000
	OU	0.0002	–	–	0.004	0.120	–	–	0.054	–	–	0.000
	EB	0.0001	–	–	0.000	0.118	–	–	–	–	–	0.000
	BMS2	0.0001	0.0001	–	–	0.089	0.311	–	0.077	0.092	–	0.001
	OUM2	0.0002	–	–	0.016	0.069	0.260	–	0.020	0.027	–	0.990
	BMS3	0.0002	0.0001	0.0001	–	−0.251	0.128	0.399	0.181	0.063	0.107	0.002
	OUM3	0.0002	–	–	0.009	−0.098	0.128	0.326	0.087	0.034	0.061	0.007
JAPr angle	BM	0.0003	–	–	–	1.411	–	–	0.122	–	–	0.000
	OU	0.0004	–	–	0.005	1.414	–	–	0.078	–	–	0.000
	EB	0.0003	–	–	0.000	1.411	–	–	–	–	–	0.000
	BMS2	0.0003	0.0004	–	–	1.353	1.742	–	0.104	0.135	–	0.002
	OUM2	0.0005	–	–	0.016	1.336	1.640	–	0.031	0.041	–	0.988
	BMS3	0.0003	0.0002	0.0005	–	0.861	1.413	1.888	0.247	0.091	0.175	0.007
	OUM3	0.0004	–	–	0.009	1.093	1.427	1.743	0.131	0.051	0.092	0.003
Joint-to-m1	BM	0.0001	–	–	–	0.410	–	–	0.056	–	–	0.000
	OU	0.0001	–	–	0.005	0.409	–	–	0.035	–	–	0.000
	EB	0.0001	–	–	0.000	0.410	–	–	–	–	–	0.000
	BMS2	0.0001	0.0001	–	–	0.430	0.224	–	0.053	0.078	–	0.009
	OUM2	0.0001	–	–	0.014	0.434	0.287	–	0.017	0.028	–	0.934
	BMS3	0.0001	0.0001	0.0001	–	0.639	0.403	0.177	0.132	0.057	0.115	0.001
	OUM3	0.0001	–	–	0.012	0.489	0.411	0.222	0.050	0.020	0.052	0.056
Body mass	BM	0.0089	–	–	–	2.000	–	–	0.616	–	–	0.027
	OU	0.0092	–	–	0.001	2.001	–	–	0.569	–	–	0.011
	EB	0.0142	–	–	−0.003	1.997	–	–	–	–	–	0.016
	BMS2	0.0110	0.0074	–	–	1.899	2.706	–	0.686	0.801	–	0.100
	OUM2	0.0092	–	–	0.001	1.872	2.736	–	0.543	0.671	–	0.023
	BMS3	0.0141	0.0053	0.0087	–	0.367	1.976	3.920	1.533	0.484	0.835	0.739
	OUM3	0.0090	–	–	0.002	0.510	2.027	3.728	1.301	0.533	0.847	0.083

Note. See Table S6 for results of analyses using nonrodent and rodent subsamples. Model parameters are the evolutionary rate of trait evolution (σ^2), trait optima (θ), and strength of attraction (α), which is also the EB rate decay parameter. The numbers after some parameters represent the different dietary regimes: faunivory (1), omnivory (2), and herbivory (3). Results are provided in the faunivory (1) columns for models in which species were not classified into different dietary regimes (i.e., BM1, OU1, and EB). See Methods for descriptions of the models. Abbreviations: A. wt., Akaike weights; BM, Brownian motion; EB, early burst; JAPr, jaw joint-angular process; m1, first lower molar; OU, Ornstein-Uhlenbeck; SE, standard error.

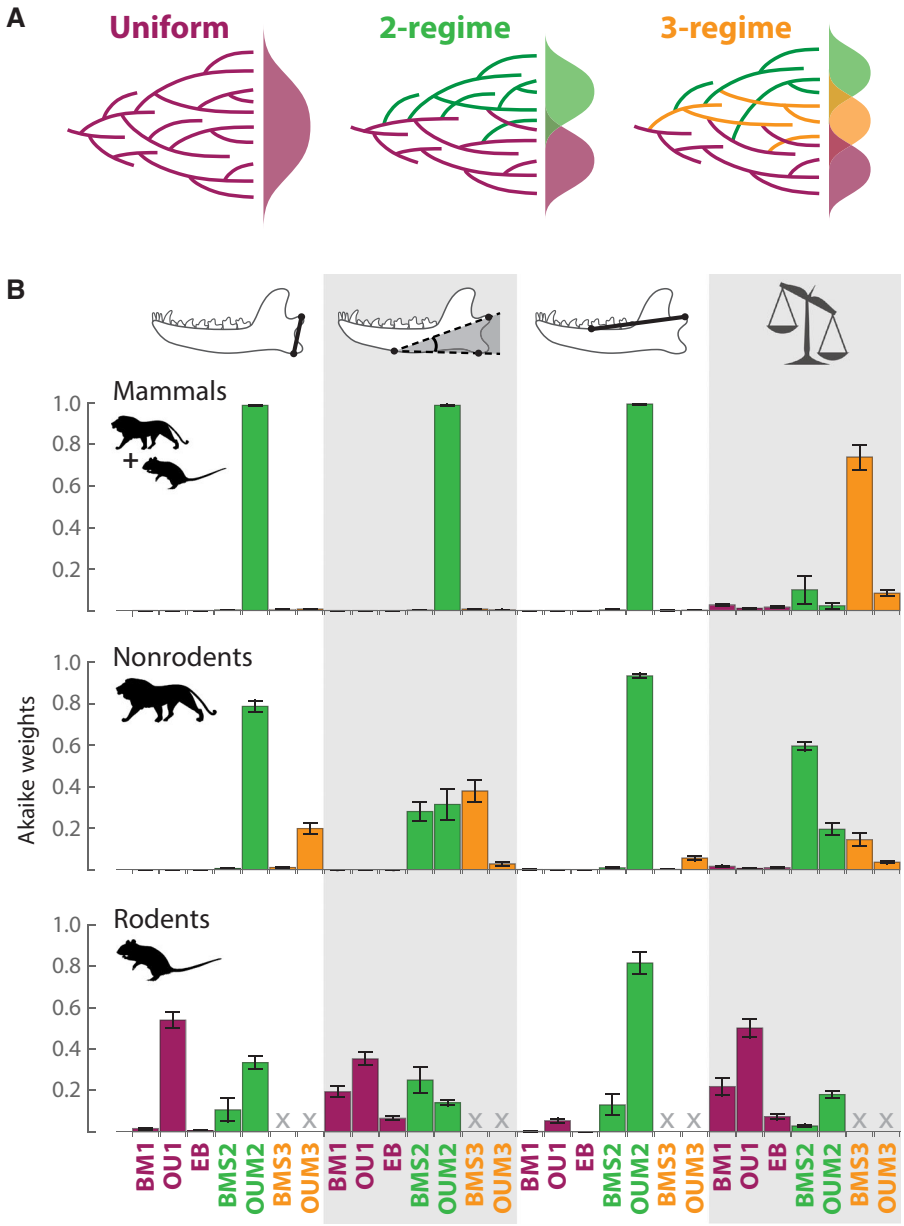

Figure 4. *A*, Conceptualizations of types of evolutionary models used in this study: uniform (maroon), two-regime (green), and three-regime (orange). Species are classified into two diets (faunivory and herbivory) for two-regime models and three diets (faunivory, omnivory, and herbivory) for three-regime models. *B*, Relative model support (Akaike weights) for the seven evolutionary models (see Methods) that were fit to jaw-joint-to-angular process (JAPr) distances, JAPr angles, jaw-joint-to-m1 distances, and body masses. Values are means of the analyses for 20 phylogenetic trees, and standard errors (whiskers) are calculated from these results. Three-regime models were not fit to rodent data because of the dearth of faunivorous species.

row length (measurement 3) and maximum erupted molar depth (measurement 8) both decrease with herbivory in nonrodents, but the trend is in the opposite direction in rodents, with both metrics increasing with herbivory. This could be due in part to many carnivorans possessing prominent carnassial molars, whereas faunivorous rodents are primarily insectivorous and have reduced molars (Helgen and Helgen 2009). An additional distinction between rodents and nonrodents is that the jaw corpus depth (measurement 7) is significantly correlated with diet in rodents but not in nonrodents (Table 1; Fig. 2; Arregoitia et al. 2017). A deeper jaw body could reflect increased incisor size for gnawing (Radinsky 1968), because the incisor alveoli extend posteriorly through the jaw corpus.

I chose to fit evolutionary models to three jaw metrics with especially strong relationships with diet: JAPr distance, JAPr angle, and jaw-joint-to-m1 distance (Table 1, Fig. 4). Although the

two JAPr metrics capture very similar morphological features of the jaw (Fig. 1), they are both analyzed here because they offer unique benefits. For instance, the JAPr angle may be less affected by subjective measurements and was independently found to be correlated with diet in a large sample of rodents (Arregoitia et al. 2017). (See extended discussion in Methods in the Supporting Information.)

Evolutionary model-fitting analyses of functional jaw morphology indicate that faunivores and herbivores occupy unique selective regimes, as two-regime models outperform all additional models for the mammal and nonrodent samples (Tables 2 and S6; Fig. 4). These results are maintained when measurement error is incorporated into the model-fitting analyses (Table S7), and when evolutionary models are fit to JAPr metrics that were size-corrected using regression residuals rather than log-shape ratios (Table S9; Fig. S4). The best fitting model for the total sample of mammals, OUM2, predicts the optimum JAPr angle (θ) to be considerably different for the two selective regimes: approximately 22 degrees for faunivores and 43 degrees for herbivores (Fig. 3C). The lack of support for three-regime models suggests the absence of a distinct adaptive peak for omnivores.

ECOMORPHOLOGICAL CONVERGENCE AMONG MAMMALIAN ORDERS

Ecomorphological convergence is a powerful indicator of adaptive evolution (Losos 2011; Zelditch et al. 2017), providing evidence that ecological specialization influences morphological evolution. The comparative analyses of this study suggest that selective pressures associated with shared diets have driven convergent evolution of jaw morphology in distantly related mammalian clades. For instance, JAPr metrics increase with herbivory in data subsets consisting of rodents, nonrodents (Table 1), and chiropterans (see Results), indicating that jaw similarities evolved convergently in each group. This is also highlighted in Figure 3B, which shows greater JAPr angles in herbivorous taxa for five major mammalian clades (rodents, carnivorans, primates, bats, and marsupials). Herbivory likely evolved independently, and often on multiple occasions, in most of these mammalian groups.

The broad taxonomic sample of this study permits the recognition of convergent jaw evolution across multiple mammalian orders. Previous studies found the JAPr distance (or a comparable metric) to be correlated with diet in carnivorans (Radinsky 1981; Figueirido et al. 2010), platyrrhine primates (Anapol and Lee 1994), ungulates (Radinsky 1985; Mendoza et al. 2002), and rodents (Arregoitia et al. 2017). However, this correlation was not especially strong in carnivorans (Radinsky 1981) or ungulates (Mendoza et al. 2002), at least relative to additional metrics, suggesting that the significant results of this study rely on sampling multiple major clades. Further, by examining morphological patterns at a broad taxonomic scale, trait variation associated with diet is expected to outweigh variation resulting from numerous additional factors that may affect jaw morphology, including functional demands due to additional uses of the jaw beyond feeding (Ross et al. 2012; Davis and Pineda-Munoz 2016).

BIOMECHANICAL LINKS BETWEEN THE ANGULAR PROCESS AND DIET

Identifying strong functional links between ecology and morphology is critical for examining the impact of ecological specialization on phenotypic diversification. Here, model-fitting analyses indicate distinct selective regimes for faunivory and herbivory, providing evidence that selection facilitates trait partitioning of jaw morphologies between these two dietary categories. However, this raises the question: what biomechanical factors are driving the dichotomy between faunivore jaws and herbivore jaws?

The JAPr metrics have a strong association with diet in all comparative analyses in this study (Tables 1, 2, S3, and S4), including supplemental analyses in which residuals from PGLS regressions against jaw length are used as size-corrected data (Table S8). The JAPr angles and distances are considerably greater in herbivores, and this pattern is independent of allometric changes related to jaw size. Thus, I focus the discussion here on biomechanical factors that are related to the mandibular angular process.

The JAPr distance can increase due to an enlarged (or depressed) angular process, which is common in many herbivorous clades (Fig. 3B). But the JAPr distance can also increase due to elevation of the jaw joint, which is especially prevalent in groups such as ungulates, primates, and lagomorphs (Table S1). These clades often use transverse grinding motions of the lower jaw during occlusion, suggesting a functional link between the elevated jaw joint and transverse movement (Greaves 1974). However, jaw joint elevation above the tooth row (measurement 4) is not as strongly correlated with diet as several additional jaw measurements (Table 1). This indicates that a shift to herbivory does not always trigger an elevation of the jaw joint, and JAPr distance is more closely linked to the size and position of the angular process.

An enlarged angular process provides greater attachment areas for the superficial masseter and medial pterygoid muscles (Fig. 1). These muscles are generally larger in herbivorous mammals (Turnbull 1970), often facilitating transverse jaw movements for grinding occlusion (Maynard Smith and Savage 1959; Radinsky 1985; Crompton et al. 2010; Grossnickle 2017). Radinsky (1985) suggested that the larger superficial masseter and medial pterygoid muscles enhanced the control of grinding action in large herbivores. Further, Grossnickle (2017) posited a link between the evolution of the angular process and jaw rotation around a dorsoventral-oriented axis (i.e., yaw), which generates transverse jaw movements. This suggests that many herbivores possess large angular processes (and attached muscles) due to masticatory jaw movements that are yaw dominated. A greater JAPr distance also

increases the moment arm lengths for the force vectors of the medial pterygoid and superficial masseter during orthal jaw closure (i.e., jaw pitch) (Maynard Smith and Savage 1959). In herbivores with proal jaw movement (e.g., many rodents), the expanded angular process may reflect lengthening of the masseter and medial pterygoid muscles, likely increasing overall muscle mass and helping maintain forceful occlusal contact during extended power strokes.

Functional trade-offs related to gape may also influence JAPr distance. Increasing the JAPr distance shifts the superficial masseter and medial pterygoid muscles farther from (i.e., more ventral to) the jaw joint, which results in increased stretch of these muscles during jaw opening (Herring and Herring 1974). This limits maximum gape and decreases bite force during wide gape, which may be especially detrimental to faunivores that consume large prey. Thus, selection pressures may favor smaller superficial masseter and medial pterygoid muscles (and shorter JAPr distances) in faunivores to permit a wider gape. Gape may also help explain why the jaw-joint-to-coronoid process distance (measurements 10) is not as strongly correlated with diet as the angular process metrics (Tables 1 and S3). The temporalis muscle inserts on the coronoid process, and it may have to remain relatively close to the jaw joint to allow a wide gape (Emerson and Radinsky 1980). This restricts faunivores from greater elevation of the coronoid process despite their relatively large temporalis muscles (Turnbull 1970).

Taken together, these biomechanical considerations suggest that functional trade-offs between faunivores and herbivores drive convergent, adaptive changes in taxa with similar diets. Enlargement of the angular process and attached musculature may decrease gape in herbivores, but it simultaneously enhances the grinding capabilities necessary for masticating plant materials. Thus, there is a strong functional link between jaw morphology and feeding ecology.

FUNCTIONAL MORPHOLOGY VERSUS BODY MASS

There are two major discrepancies between results for functional jaw morphology and body mass. First, several jaw metrics that capture important functional traits (e.g., angular process size) outperform body mass as predictors of diet (Table 1; Figs. 2 and 3). This result is particularly apparent in Figure 3, which shows a distinct separation of JAPr angles between herbivores and faunivores (Fig. 3C), whereas body masses of the two dietary groups show considerable overlap (Fig. 3D). Thus, dietary specialization during the diversification of therian mammals appears to have generated greater trait partitioning in functional morphologies than in body mass.

The second major discrepancy between results for jaw morphology and body mass is that jaw shape shows less variance within dietary categories (Figs. 2–4), and the support for OU models (vs. BM models for body mass) indicate that feeding ecology generates greater selective pressures on jaw morphology. Further, three functionally relevant jaw metrics (JAPr distance, JAPr angle, and joint-to-m1 distance) are all best explained by two-regime (i.e., faunivory and herbivory) models, whereas body mass data are best explained by three-regime (i.e., faunivory, omnivory, and herbivory) models (Table 2; Fig. 4; Price and Hopkins 2015). Thus, feeding ecology has fundamentally unique effects on functional jaw morphology and body mass.

A concern is that I differentiate diets by the proportion of plant material, which is simplistic (especially because plant materials can vary considerably in their physical and nutritional properties) and may not capture nuanced differences among more specific dietary categories (Pineda-Munoz and Alroy 2014; Davis and Pineda-Munoz 2016). Pineda-Munoz et al. (2016) separate mammals into a larger number of dietary groups, and they found distinct body size patterns related to dietary preference in mammals. For instance, subcategories within faunivores (e.g., insectivores and carnivores) and herbivores (e.g., frugivores and granivores) have unique body mass distributions (Eisenberg 1981; Pineda-Munoz et al. 2016). Thus, if diet is a major driver of body mass evolution, it is likely due to the presence of many local adaptive peaks (or subzones within larger adaptive zones) associated with specific diets (Zelditch et al. 2017), rather than an adaptive landscape that is dominated by two or three peaks, as tested in this study. Future work can explore this possibility by examining a greater number of dietary categories using large-scale datasets.

These considerations suggest two potential explanations for the discrepancies between the macroevolutionary patterns of jaw shape and body mass. First, the adaptive landscape associated with body mass is more complex than that of functional jaw morphology (Slater 2015). Although jaw analyses suggest two major adaptive peaks for jaw morphology (Fig. 4), the adaptive landscape for body mass may include many adaptive peaks that are associated with more-specific dietary guilds than the three categories of this study (Pineda-Munoz et al. 2016; Zelditch et al. 2017). Further, these peaks may not be stationary through time, and fluctuating peaks could generate macroevolutionary patterns that resemble BM processes (Revell et al. 2008), which is congruent with the support for BM models for body mass (Table 2; Fig. 4). This complexity is also compounded by the numerous factors beyond diet that influence body mass, such as life-history traits, habitat (e.g., terrestrial vs. aquatic), climate, predation pressures, biogeography, and extinction risk (Eisenberg 1981; Peters 1986; Brown and Maurer 1989; Tomiya 2013; Smits 2015; Gearty et al. 2018). Selective pressures associated with these factors may oppose the pressures generated by dietary ecology, weakening the observed correlation between diet and body mass.

A second explanation for the discrepancies between results for jaw shape and body mass is that size is more evolutionarily labile than functional morphology. Body mass changes may be

the "evolutionary path of least resistance" when mammalian lineages first shift to new diets (Marroig and Cheverud 2005). This could result in body mass diversification within clades during early stages of ecological diversification events (Raia et al. 2012), especially in lower level clades (Marroig and Cheverud 2005; Mahler et al. 2010; Uyeda et al. 2011), small mammals (Smith et al. 2004; Zelditch et al. 2017), and situations in which shifts in body size facilitate a greater range of dietary options (e.g., an increase in size allows faunivores to consume larger prey; Santana and Cheung 2016). In contrast, functional morphology may be less evolutionarily labile, such that substantial evolutionary changes only occur with sustained, strong selective pressures. For instance, evolutionary changes in jaw shape may be inhibited by the need for concurrent modifications in associated soft tissues and complex chewing cycles. However, eventual evolutionary changes to the masticatory apparatus may help facilitate occupation of new adaptive zones/peaks, subsequently resulting in stabilizing selection that will constrain the variance of functional morphologies within those zones (Simpson 1944; Santana and Cheung 2016; Slater and Friscia 2019). This idea is supported by the relatively strong fit of multi-regime OU models to functional jaw morphology (Tables 2 and S9; Figs. 4 and S4), because evidence for an OU process is often linked to stabilizing selection (Hansen 1997; Butler and King 2004; Hunt 2007).

Despite the distinct results for jaw shape and body mass, neither trait supports an "early burst" in morphological divergence in therian mammals (Fig. 4; Tables 2, S6, and S9). This is consistent with paleontological evidence that also contradicts an "early burst" at the therian phylogenetic node. The early therian lineages in the Late Jurassic–Early Cretaceous (ca. 160–100 million years ago) were primarily small insectivores, and therians do not show evidence of significant ecological diversification until the Late Cretaceous (Grossnickle and Newham 2016; Grossnickle et al. 2019). Thus, early therians may not have experienced an "early burst" in functional morphology, but many therian subclades likely underwent rapid ecological diversification in the latest Cretaceous and early Cenozoic (Alroy 1999; Smith et al. 2010; Raia et al. 2013; Slater 2013; Halliday and Goswami 2016; Grossnickle and Newham 2016; Grossnickle et al. 2019; Slater and Friscia 2019).

ECOLOGICAL SURROGATES IN MACROEVOLUTIONARY STUDIES

Conclusions about macroevolutionary patterns in therians are sensitive to the ecomorphological trait being examined, and I advocate using functionally relevant traits as ecomorphological correlates when possible (Slater 2015; Smits 2015; Santana and Cheung 2016; Chen et al. 2019; Slater and Friscia 2019). Evolutionary patterns for these functional traits provide direct evidence of selective pressures associated with specific ecological or biomechanical functions. In contrast, many factors influence body mass, and therefore it may be difficult to decipher which ecological factors are specifically driving evolutionary patterns.

A prerequisite for using functional morphologies as ecological proxies, however, is the identification of ecomorphological traits that can be applied to higher level clades. Strong links between tooth morphology and diet have been previously established in mammals (Evans et al. 2007; Boyer 2008; Christensen 2014; Pineda-Munoz et al. 2017; Berthaume et al. 2019), proving to be especially valuable for paleontological studies (Van Valkenburgh 1988; Janis 1995; Wilson et al. 2012; Slater 2015; Grossnickle and Newham 2016; Chen et al. 2019). The jaw correlates of diet presented in this study, especially JAPr distance and JAPr angle, may offer new functional traits that can be easily applied to broad studies of extant and fossil mammals.

Conclusions

Ecological traits can have various evolutionary influences on different morphological traits. Here, I examine the evolutionary influence of feeding ecology on functional jaw morphology and body mass in therian mammals, a clade that has experienced considerable ecological diversification over the past 100 million years. I identify several jaw traits that are significantly influenced by diet (Table 1) and convergently evolved among major mammalian clades (Figs. 2 and 3). An especially strong predictor of diet is the distance between the jaw joint and the angular process (JAPr distance), which shows considerable trait partitioning (Table 2; Figs. 2–4) due to strong selective pressures associated with functional trade-offs between herbivores and faunivores (Maynard Smith and Savage 1959; Turnbull 1970; Herring and Herring 1974; Grossnickle 2017). Further, jaw metrics such as JAPr distance and joint-to-m1 distance outperform body mass as predictors of diet (Table 1; Figs. 2 and 3), suggesting that diet-related selective pressures have acted more forcibly on functional morphology than on body size during the ecological radiation of therians. Results also highlight the complexity of body mass evolution (Tables 2 and S6; Fig. 4; Pineda-Munoz et al. 2016), which is influenced by many factors beyond diet. Body mass may be evolutionarily labile in relation to functional morphology (Marroig and Cheverud 2005; Slater and Friscia 2019), and it may be the evolutionary path of least resistance when a clade initially diversifies ecologically. However, sustained selective pressures will eventually generate more substantial trait partitioning in functional morphologies than in body masses.

Ecological specialization is a central driver of phenotypic diversification. However, the impact of ecological pressures can vary among different morphological traits (e.g., size and shape), and observed macroevolutionary patterns within a clade are sensitive to the ecomorphological traits being examined (Fig. 4;

Wainwright 2007; Harmon et al. 2010; Slater 2015; Santana and Cheung 2016; Slater and Friscia 2019). This highlights the importance of identifying strong associations between functional morphologies and ecologies, especially because morphological traits can serve as valuable ecological surrogates in macroevolutionary, macroecological, and paleoenvironmental studies (Wilson et al. 2012; Grossnickle and Polly 2013; Slater 2015; Vermillion et al. 2018; Chen et al. 2019). The jaw metrics identified here offer an additional ecomorphological correlate beyond those commonly found in the literature (e.g., dental metrics) that can be readily applied to extant and fossil mammals.

AUTHOR CONTRIBUTIONS

DMG designed and conducted all the research in this study.

ACKNOWLEDGMENTS

This project was enriched by feedback from G. J. Slater, K. D. Angielczyk, C. F. Ross, Z.-X. Luo, M. I. Coates, P. D. Polly, J. Iriarte-Diaz, D. Krentzel, L. N. Weaver, G. P. Wilson, J. Claytor, A. K. Bormet, and two anonymous reviewers. N. S. Upham graciously provided early access to the phylogenetic trees used in this study. For access to Field Museum of Natural History (FMNH) and Smithsonian National Museum of Natural History specimens, I thank B. D. Patterson, L. R. Heaney, A. W. Ferguson, H. F. James, and D. P. Lunde. M. Chen kindly supplied jaw photographs of several specimens, and I thank P. Myers for providing jaw photographs via the University of Michigan Museum of Zoology Animal Diversity Web. Funding was from the FMNH (Brown Graduate Fellowship), the University of Chicago (William Rainey Harper Fellowship), University of Washington (Hell Creek Project Postdoctoral Research Fellowship), and the National Science Foundation Postdoctoral Research Fellowship in Biology (DBI-1812126).

DATA ARCHIVING

All data are included in Table S1 of the Supporting Information and archived in Dryad (https://doi.org/10.5061/dryad.573n5tb40).

CONFLICT OF INTEREST

The author declares no conflict of interest.

LITERATURE CITED

Ahrens, D., J. Schwarzer, and A. P. Vogler. 2014. The evolution of scarab beetles tracks the sequential rise of angiosperms and mammals. Proc. R. Soc. B Biol. Sci 281:20141470.

Akaike, H. 1974. A new look at the statistical model identification. IEEE Trans. Automat. Contr. 19:716–723.

Alroy, J. 1999. The fossil record of North American mammals: evidence for a Paleocene evolutionary radiation. Syst. Biol 48:107–118.

Anapol, F., and S. Lee. 1994. Morphological adaptation to diet in platyrrhine primates. Am. J. Phys. Anthropol. 94:239–261.

Arregoitia, L. D. V., D. O. Fisher, and M. Schweizer. 2017. Morphology captures diet and locomotor types in rodents. R. Soc. Open Sci. 4:160957.

Beaulieu, J. M., and B. O'Meara. 2016. OUwie: analysis of evolutionary rates in an OU framework. R package, version 1.49. R Foundation for Statistical Computing, Vienna, Austria.

Berthaume, M. A., J. Winchester, and K. Kupczik. 2019. Ambient occlusion and PCV (portion de ciel visible): a new dental topographic metric and proxy of morphological wear resistance. PLoS ONE 14:e0215436.

Boyer, D. M. 2008. Relief index of second mandibular molars is a correlate of diet among prosimian primates and other euarchontan mammals. J. Human Evol. 55:1118–1137.

Brown, J. H., and B. A. Maurer. 1989. Macroecology: the division of food and space among species on continents. Science 243:1145–1150.

Butler, M. A., and A. A. King. 2004. Phylogenetic comparative analysis: a modeling approach for adaptive evolution. Am. Nat. 164:683–695.

Chen, M., C. A. Strömberg, and G. P. Wilson. 2019. Assembly of modern mammal community structure driven by Late Cretaceous dental evolution, rise of flowering plants, and dinosaur demise. Proc. Natl. Acad. Sci. USA 116:9931–9940.

Cheverud, J. M. 1982. Phenotypic, genetic, and environmental morphological integration in the cranium. Evolution 36:499–516.

Christensen, H. B. 2014. Similar associations of tooth microwear and morphology indicate similar diet across marsupial and placental mammals. PLoS ONE 9:e102789.

Claude, J. 2013. Log-shape ratios, Procrustes superimposition, elliptic Fourier analysis: three worked examples in R. Hystrix, It. J. Mamm. 24:94–102.

Collinson, M. E., and J. J. Hooker. 1991. Fossil evidence of interactions between plants and plant-eating mammals. Philos. Trans. R. Soc. Lon. B Biol. Sci. 333:197–208.

Cooper, N., and A. Purvis. 2010. Body size evolution in mammals: complexity in tempo and mode. Am. Nat. 175:727–738.

Cooper, N., G. H. Thomas, C. Venditti, A. Meade, and R. P. Freckleton. 2016. A cautionary note on the use of Ornstein Uhlenbeck models in macroevolutionary studies. Biol. J. Linn. Soc. 118:64–77.

Cox, P. G., and H. Baverstock. 2016. Masticatory muscle anatomy and feeding efficiency of the American beaver, *Castor canadensis* (Rodentia, Castoridae). J. Mamm. Evol. 23:191–200.

Crompton, A. W., T. Owerkowicz, and J. Skinner. 2010. Masticatory motor pattern in the koala (*Phascolarctos cinereus*): a comparison of jaw movements in marsupial and placental herbivores. J. Exp. Zool. A Ecol. Genet. Physiol. 313:564–578.

Darwin, C. 1859. On the origin of species by means of natural selection. John Murray, Lond.

Davis, M., and S. Pineda-Munoz. 2016. The temporal scale of diet and dietary proxies. Ecol. Evol. 6:1883–1897.

Demment, M. W., and P. J. Van Soest. 1985. A nutritional explanation for body-size patterns of ruminant and nonruminant herbivores. Am. Nat. 125:641–672.

Eisenberg, J. F. 1981. The mammalian radiations: an analysis of trends in evolution, adaptation, and behaviour. Chicago Univ. Press, Chicago.

Emerson, S. B., and L. Radinsky. 1980. Functional analysis of sabertooth cranial morphology. Paleobiology 6:295–312.

Eriksson, O. 2016. Evolution of angiosperm seed disperser mutualisms: the timing of origins and their consequences for coevolutionary interactions between angiosperms and frugivores. Biol. Rev. Camb. Philos. Soc. 91:168–186.

Evans, A. R., D. Jones, A. G. Boyer, J. H. Brown, D. P. Costa, S. K. Ernest, E. M. Fitzgerald, M. Fortelius, J. L. Gittleman, M. J. Hamilton, et al. 2012. The maximum rate of mammal evolution. Proc. Natl. Acad. Sci. USA 109:4187–4190.

Evans, A. R., G. P. Wilson, M. Fortelius, and J. Jernvall. 2007. High-level similarity of dentitions in carnivorans and rodents. Nature 445:78–81.

Faurby, S., M. Davis, R. Pedersen, S. D. Schowanek, A. Antonelli, and J. C. Svenning. 2018. PHYLACINE 1.2: the phylogenetic atlas of mammal macroecology. Ecology 99:2626–2626.

Feild, T. S., T. J. Brodribb, A. Iglesias, D. S. Chatelet, A. Baresch, G. R. Upchurch Jr., B. Gomez, B. A. R. Mohr, C. Coiffard, J. Kvacek, et al. 2011. Fossil evidence for Cretaceous escalation in angiosperm leaf vein evolution. Proc. Natl. Acad. Sci. USA 108:8363–8366.

Figueirido, B., F. J. Serrano-Alarcon, G. J. Slater, and P. Palmqvist. 2010. Shape at the cross-roads: homoplasy and history in the evolution of the carnivoran skull towards herbivory. J. Evol. Biol. 23:2579–2594.

Garland, T., Jr., A. W. Dickerman, C. M. Janis, and J. A. Jones. 1993. Phylogenetic analysis of covariance by computer simulation. Syst. Biol. 42:265–292.

Gearty, W., C. R. McClain, and J. L. Payne. 2018. Energetic tradeoffs control the size distribution of aquatic mammals. Proc. Natl. Acad. Sci. USA 115:4194–4199.

Grafen, A. 1989. The phylogenetic regression. Philos. Trans. R. Soc. Lon. B Biol. Sci. 326:119–157.

Graham, H. M. 2003. Confronting multicollinearity in ecological multiple regression. Ecology 84:2809–2815.

Greaves, W. S. 1974. Functional implications of mammalian jaw joint position. Forma et Functio 7:363–376.

Grossnickle, D. M. 2017. The evolutionary origin of jaw yaw in mammals. Sci. Rep. 7:45094.

Grossnickle, D. M., and E. Newham. 2016. Therian mammals experience an ecomorphological radiation during the Late Cretaceous and selective extinction at the K–Pg boundary. Proc. R. Soc. B Biol. Sci. 283: 20160256.

Grossnickle, D. M., and P. D. Polly. 2013. Mammal disparity decreases during the Cretaceous angiosperm radiation. Proc. R. Soc. B Biol. Sci. 280:20132110.

Grossnickle, D. M., S. M. Smith, and G. P. Wilson. 2019. Untangling the multiple ecological radiations of early mammals. Trends Ecol. Evol. https://doi.org/10.1016/j.tree.2019.05.008.

Halliday, T. J. D., and A. Goswami. 2016. Eutherian morphological disparity across the end-Cretaceous mass extinction. Biol. J. Linn. Soc. Lond. 118:152–168.

Hansen, T. F. 1997. Stabilizing selection and the comparative analysis of adaptation. Evolution 51:1341–1351.

Harmon, L. J., J. B. Losos, T. J. Davies, R. G. Gillespie, J. L. Gittleman, W. B. Jennings, K. H. Kozak, M. A. McPeek, F. Moreno-Roark, T. J. Near, et al. 2010. Early bursts of body size and shape evolution are rare in comparative data. Evolution 64:2385–2396.

Helgen, K. M., and L. E. Helgen. 2009. Biodiversity and biogeography of the moss-mice of New Guinea: a taxonomic revision of *Pseudohydromys* (Muridae: Murinae). Bull. Am. Mus. Nat. Hist. 331:230–313.

Herring, S. W., and S. E. Herring. 1974. The superficial masseter and gape in mammals. Am. Nat. 108:561–576.

Hopkins, S. S. 2018. Estimation of body size in fossil mammals. Pp. 7–22 *in* D. A. Croft, D. F. Su, and S. W. Simpson, eds. Methods in paleoecology: reconstructing Cenozoic terrestrial environments and ecological communities. Springer Nature Switzerland, Cham, Switzerland.

Huang, S., J. T. Eronen, C. M. Janis, J. J. Saarinen, D. Silvestro, and S. A. Fritz. 2017. Mammal body size evolution in North America and Europe over 20 Myr: similar trends generated by different processes. Proc. R. Soc. B Biol. Sci. 284:20162361.

Hunt, G. 2007. The relative importance of directional change, random walks, and stasis in the evolution of fossil lineages. Proc. Natl. Acad. Sci. USA 104:18404–18408.

Hurvich, C. M., and C. L. Tsai. 1989. Regression and time series model selection in small samples. Biometrika 76:297–307.

Janis, C. M. 1995. Correlations between craniodental morphology and feeding behavior in ungulates: reciprocal illumination between living and fossil taxa. Pp. 76–98 *in* J. J. Thomason, ed. Functional morphology in vertebrate paleontology. Cambridge Univ. Press, Cambridge, UK.

Jernvall, J., J. P. Hunter, and M. Fortelius. 1996. Molar tooth diversity, disparity, and ecology in Cenozoic ungulate radiations. Science 274:1489–1492.

Jones, K. E., et al. 2009. PanTHERIA: a species-level database of life history, ecology, and geography of extant and recently extinct mammals. Ecology 90:2648–2648.

Lande, R., and S. J. Arnold. 1983. The measurement of selection on correlated characters. Evolution 37:1210–1226.

Lazagabaster, I. A., J. Rowan, J. M. Kamilar, and K. E. Reed. 2016. Evolution of craniodental correlates of diet in African Bovidae. J. Mamm. Evol. 23:385–396.

Losos, J. B. 2011. Convergence, adaptation, and constraint. Evolution 65:1827–1840.

Luo, Z. X., C. X. Yuan, Q. J. Meng, and Q. Ji. 2011. A Jurassic eutherian mammal and divergence of marsupials and placentals. Nature 476:442–445.

Maestri, R., B. D. Patterson, R. Fornel, L. R. Monteiro, and T. R. O. Freitas. 2016. Diet, bite force and skull morphology in the generalist rodent morphotype. J. Evol. Biol. 29:2191–2204.

Mahler, D. L., L. J. Revell, R. E. Glor, and J. B. Losos. 2010. Ecological opportunity and the rate of morphological evolution in the diversification of Greater Antillean anoles. Evolution 64:2731–2745.

Marroig, G., and J. M. Cheverud. 2005. Size as a line of least evolutionary resistance: diet and adaptive morphological radiation in New World monkeys. Evolution 59:1128–1142.

Maynard Smith, J., and R. J. G. Savage. 1959. The mechanics of mammalian jaws. School Sci. Rev. 141:289–301.

McKenna, D. D., A. S. Sequeira, A. E. Marvaldi, and B. D. Farrell. 2009. Temporal lags and overlap in the diversification of weevils and flowering plants. Proc. Natl. Acad. Sci. USA 106:7083–7088.

McShea, D. W. 1994. Mechanisms of large-scale evolutionary trends. Evolution 48:1747–1763.

Meloro, C., and P. O'Higgins. 2011. Ecological adaptations of mandibular form in fissiped Carnivora. J. Mamm. Evol. 18:185–200.

Mendoza, M., C. M. Janis, and P. Palmqvist. 2002. Characterizing complex craniodental patterns related to feeding behaviour in ungulates: a multivariate approach. J. Zool. 258:223–246.

Meng, Q. J., D. M. Grossnickle, D. Liu, Y. G. Zhang, A. I. Neander, Q. Ji, and Z. X. Luo. 2017. New gliding mammaliaforms from the Jurassic. Nature 548:291–296.

Mitchell, J. S., and P. J. Makovicky. 2014. Low ecological disparity in Early Cretaceous birds. Proc. R. Soc. B Biol. Sci. 281:20140608.

Monteiro, L. R., and M. R. Nogueira. 2011. Evolutionary patterns and processes in the radiation of phyllostomid bats. BMC Evol. Biol. 11:137–159.

Mosimann, J. E. 1970. Size allometry: size and shape variables with characterizations of the lognormal and generalized gamma distributions. J. Am. Stat. Assoc. 65:930–945.

Moreau, C. S., C. D. Bell, R. Vila, S. B. Archibald, and N. E. Pierce. 2006. Phylogeny of the ants: diversification in the age of angiosperms. Science 312:101–104.

Myers, P., R. Espinosa, C. S. Parr, T. Jones, G. S. Hammond, and T. A. Dewey. 2017. The animal diversity web. Available via http://animaldiversity.org.

Nogueira, M. R., L. R. Monteiro, A. L. Peracchi, and A. F. de Araújo. 2005. Ecomorphological analysis of the masticatory apparatus in the seed-eating bats, genus *Chiroderma* (Chiroptera: Phyllostomidae). J. Zool. 266:355–364.

Nowak, R. M. 1999. Walker's mammals of the world. Johns Hopkins Univ. Press, Baltimore, MD.

Olsen, A. M. 2017. Feeding ecology is the primary driver of beak shape diversification in waterfowl. Funct. Ecol. 31:1985–1995.

Osborn, H. F. 1902. The law of adaptive radiation. Am. Nat. 36:353–363.

Paradis, E., J. Claude, and K. Strimmer. 2004. APE: analyses of phylogenetics and evolution in R language. Bioinformatics 20:289–290.

Pennell, M. W., J. M. Eastman, G. J. Slater, J. W. Brown, J. C. Uyeda, R. G. FitzJohn, M. E. Alfaro, L. J. Harmon. 2014. geiger v2.0: an expanded suite of methods for fitting macroevolutionary models to phylogenetic trees. Bioinformatics 30:2216–2218.

Peters, R. H. 1986. The ecological implications of body size. Vol. 2. Cambridge Univ. Press, Cambridge, UK.

Pineda-Munoz, S., and J. Alroy. 2014. Dietary characterization of terrestrial mammals. Proc. R. Soc. B Biol. Sci. 281:20141173.

Pineda-Munoz, S., A. R. Evans, and J. Alroy. 2016. The relationship between diet and body mass in terrestrial mammals. Paleobiology 42: 659–669.

Pineda-Munoz, S., I. A. Lazagabaster, J. Alroy, and A. R. Evans. 2017. Inferring diet from dental morphology in terrestrial mammals. Methods Ecol. Evol. 8:481–491.

Pinheiro, J., D. Bates, S. DebRoy, and D. Sarkar. 2016. nlme: linear and nonlinear mixed effects models. R package, version 3.1-128. R Foundation for Statistical Computing, Vienna, Austria.

Price, S. A., and S. S. Hopkins. 2015. The macroevolutionary relationship between diet and body mass across mammals. Biol. J. Linn. Soc. Lond. 115:173–184.

Price, S. A., S. T. Friedman, K. A. Corn, C. M. Martinez, O. Larouche, and P. C. Wainwright. 2019. Building a body shape morphospace of teleostean fishes. Integr. Comp. Biol. 59:716–730.

R Core Team. 2016. R: A language and environment for statistical computing. R Foundation for Statistical Computing, Vienna, Austria.

Radinsky, L. B. 1968. A new approach to mammalian cranial analysis, illustrated by examples of prosimian primates. J. Morphol. 124:167–179.

———. 1981. Evolution of skull shape in carnivores: 1. Representative modern carnivores. Biol. J. Linn. Soc. 15:369–388.

———. 1985. Approaches in evolutionary morphology: a search for patterns. Annu. Rev. Ecol. Syst. 16:1–14.

Raia, P., F. Carotenuto, F. Passaro, D. Fulgione, and M. Fortelius. 2012. Ecological specialization in fossil mammals explains Cope's rule. Am. Nat. 179:328–337.

Raia, P., F. Carotenuto, F. Passaro, P. Piras, D. Fulgione, L. Werdelin, J. Saarinen, and M. Fortelius. 2013. Rapid action in the Palaeogene, the relationship between phenotypic and taxonomic diversification in Coenozoic mammals. Proc. R. Soc. B Biol. Sci. 280:20122244.

Raup, D. M., and S. J. Gould. 1974. Stochastic simulation and evolution of morphology-towards a nomothetic paleontology. Syst. Biol. 23:305–322.

Revell, L. J. 2009. Size-correction and principal components for interspecific comparative studies. Evolution 63:3258–3268.

———. 2010. Phylogenetic signal and linear regression on species data. Methods Ecol. Evol 1:319–329.

———. 2012. phytools: an R package for phylogenetic comparative biology (and other things). Methods Ecol. Evol. 3:217–223.

Revell, L. J., L. J. Harmon, and D. C. Collar. 2008. Phylogenetic signal, evolutionary process, and rate. Syst. Biol. 57:591–601.

Ross, C. F., J. Iriarte-Diaz, and C. L. Nunn. 2012. Innovative approaches to the relationship between diet and mandibular morphology in primates. Int. J. Primatol. 33:632–660.

Saarinen, J. J., A. G. Boyer, J. H. Brown, D. P. Costa, S. K. M. Ernest, A. R. Evans, M. Fortelius, J. L. Gittleman, M. J. Hamilton, L. E. Harding, et al. 2014. Patterns of maximum body size evolution in Cenozoic land mammals: eco-evolutionary processes and abiotic forcing. Proc. R. Soc. B Biol. Sci. 281:20132049.

Santana, S. E., and E. Cheung. 2016. Go big or go fish: morphological specializations in carnivorous bats. Proc. R. Soc. B Biol. Sci. 283: 20160615.

Schneider, C. A., W. S. Rasband, and K. W. Eliceiri. 2012. NIH Image to ImageJ: 25 years of image analysis. Nat. Methods 9:671–675.

Seilacher, A. 1970. Arbeitskonzept zur konstruktions-morphologie. Lethaia 3:393–396.

Simpson, G. G. 1944. Tempo and mode in evolution. Columbia Univ. Press, New York.

———. 2013. Phylogenetic evidence for a shift in the mode of mammalian body size evolution at the Cretaceous-Palaeogene boundary. Methods Ecol. Evol. 4:734–744.

———. 2015. Iterative adaptive radiations of fossil canids show no evidence for diversity-dependent trait evolution. Proc. Natl. Acad. Sci. USA 112:4897–4902.

Slater, G. J., and A. R. Friscia. 2019. Hierarchy in adaptive radiation: a case study using the Carnivora (Mammalia). Evolution 73:524–539.

Smith, F. A., and S. K. Lyons. 2011. How big should a mammal be? A macroecological look at mammalian body size over space and time. Philos. Trans. R. Soc. Lon. B Biol. Sci. 366:2364–2378.

Smith, F. A., A. G. Boyer, J. H. Brown, D. P. Costa, T. Dayan, S. K. M. Ernest, A. R. Evans, M. Fortelius, J. L. Gittleman, M. J. Hamilton, et al. 2010. The evolution of maximum body size of terrestrial mammals. Science 330:1216–1219.

Smith, F. A., J. H. Brown, J. P. Haskell, S. K. Lyons, J. Alroy, E. L. Charnov, T. Dayan, B. J. Enquist, S. K. Ernest, E. A. Hadly, et al. 2004. Similarity of mammalian body size across the taxonomic hierarchy and across space and time. Am. Nat. 163:672–691.

Smits, P. D. 2015. Expected time-invariant effects of biological traits on mammal species duration. Proc. Natl. Acad. Sci. USA 112:13015–13020.

Sokal, R. R., and F. J. Rohlf. 1995. Biometry: the principles and practice of statistics in biological research. W. H. Freeman and Company, New York.

Thomas, G. H., R. P. Freckleton, and T. Székely. 2006. Comparative analyses of the influence of developmental mode on phenotypic diversification rates in shorebirds. Proc. R. Soc. B Biol. Sci. 273:1619–1624.

Tomiya, S. 2013. Body size and extinction risk in terrestrial mammals above the species level. Am. Nat. 182:E196–E214.

Turnbull, W. D. 1970. Mammalian masticatory apparatus. Fieldiana Geol. 18:149–356.

Upham, N., J. A. Esselstyn, and W. Jetz. 2019. Inferring the mammal tree: species-level sets of phylogenies for questions in ecology, evolution, and conservation. PLoS Biol. 17:e3000494.

Uyeda, J. C., T. F. Hansen, S. J. Arnold, and J. Pienaar. 2011. The million-year wait for macroevolutionary bursts. Proc. Natl. Acad. Sci. USA 108:15908–15913.

Van Valkenburgh, B. 1988. Trophic diversity in past and present guilds of large predatory mammals. Paleobiology 14:155–173.

Venditti, C., A. Meade, and M. Pagel. 2011. Multiple routes to mammalian diversity. Nature 479:393–396.

Vermillion, W. A., P. D. Polly, J. J. Head, J. T. Eronen, and A. M. Lawing. 2018. Ecometrics: a trait-based approach to paleoclimate and paleoenvironmental reconstruction. Pp. 373–394 *in* D. A. Croft, D. F. Su, and S. W. Simpson, eds. Methods in paleoecology: reconstructing Cenozoic terrestrial environments and ecological communities. Springer Nature Switzerland, Cham, Switzerland.

von Koenigswald, W., U. Anders, S. Engels, J. A. Schultz, and O. Kullmer. 2013. Jaw movement in fossil mammals: analysis, description and visualization. Paläontologische Zeitschrift 87:141–159.

Wainwright, P. C. 2007. Functional versus morphological diversity in macroevolution. Annu. Rev. Ecol. Evol. Syst. 38:381–401.

Wilson, G. P., A. R. Evans, I. J. Corfe, P. D. Smits, M. Fortelius, and J. Jernvall. 2012. Adaptive radiation of multituberculate mammals before the extinction of dinosaurs. Nature 483:457–460.

Wing, S. L., and B. H. Tiffney. 1987. The reciprocal interaction of angiosperm evolution and tetrapod herbivory. Rev. Palaeobot. Palynol. 50:179–210.

Wright, S. 1932. The roles of mutation, inbreeding, crossbreeding, and selection in evolution. Pp. 356–366 *in* D. F. Jones, ed.Proceedings of the Sixth International Congress of Genetics. Blackwell Publishing, Hoboken, NJ.

Zelditch, M. L., J. Ye, J. S. Mitchell, and D. L. Swiderski. 2017. Rare ecomorphological convergence on a complex adaptive landscape: Body size and diet mediate evolution of jaw shape in squirrels (Sciuridae). Evolution 71:633–649.

Associate Editor: M. Cardillo
Handling Editor: M. R. Servedio

Supporting Information

Additional supporting information may be found online in the Supporting Information section at the end of the article.

Table S2. Descriptions of jaw measurements, which are also displayed in Figure 1.

Table S3. Summary statistics for the multiple PGLS regression, using seven jaw measurements (of the original 13) and body mass as predictors of diet.

Table S4. Best-performing models (ΔAICc < 2) of multiple PGLS regression using various combinations of jaw measurements (Fig. 1, Table S2) and body mass.

Table S5. Phylogenetic one-way analyses of variance (pANOVAs), using three alternative definitions for categorizing species into discrete diets (see text).

Table S6 (page 15). Fits of evolutionary models to JAPr distances, JAPr angles, jaw-joint-to-m1 distances, and body masses for nonrodents (top) and rodents (bottom).

Table S7. Model support (via Akaike weights) for evolutionary models fit to morphological data for analyses in which measurement error is included (left column) and excluded (right column, from Table 2).

Table S8. Summary statistics for phylogenetic one-way analyses of variance (pANOVAs) and bivariate phylogenetic generalized least squares (PGLS) regressions, examining the relationship between diet and jaw shape in mammals.

Table S9. Fits of evolutionary models to mammalian JAPr distances (measurement 12) and JAPr angles (measurement 13), using residuals from PGLS regressions of jaw measurements against jaw length (i.e. the alternative size-correction method; see Supplementary Results).

Figure S1. Derived jaw morphologies of select mammalian species.

Figure S2. Histograms of JAPr distances (*A*) and jaw-joint-to-m1 distances (*B*), displaying the frequency of faunivorous species (maroon) and herbivorous species (green).

Figure S3. Schematic jaw images of nonrodents (*A*) and rodents (*B*), displaying major morphological changes that are driven by differences in diet.

Figure S4. Relative model support (Akaike weights) for the seven evolutionary models (see Methods) that were fit to jaw-joint-to-angular process (JAPr) distances and JAPr angles.

TABLE S1. Measurements: See Figure 1 and Table S2 for descriptions of the 13 jaw and molar measurements.